THE NEUROPATHOLOGICAL EFFECTS OF ZINC AND COPPER SUPPLEMENTATION ON A DUAL TRANSGENIC (HAPP/HTAU) MOUSE MODEL OF ALZHEIMER'S DISEASE

by

Rafael Hoyos Justiniano

A Thesis
Submitted to the
Graduate Faculty
of
George Mason University
in Partial Fulfillment of
The Requirements for the Degree
of
Master of Arts
Psychology

Committee:

_____ Director

_____

_____

_____ Department Chairperson

_____ Dean, College of Humanities and Social Sciences

Date: _____ Summer Semester 2022
George Mason University
Fairfax, VA

The Neuropathological Effects of Zinc and Copper Supplementation on a Dual Transgenic (hAPP/htau) Mouse Model of Alzheimer's Disease

A Thesis submitted in partial fulfillment of the requirements for the degree of Master of Arts at George Mason University

by

Rafael Hoyos Justiniano
Bachelor of Science
George Mason University, 2020

Director: Jane M. Flinn, Associate Professor
Department of Psychology

Summer Semester 2022
George Mason University
Fairfax, VA

DEDICATION

This thesis is dedicated to my family and to those who have supported me through my academic journey.

ACKNOWLEDGEMENTS

I would like to thank the members of my committee: Dr. Flinn, Dr. Grant, and Dr. Murdoch for lending me their expertise and guidance throughout this process.

I would like to thank my family for their unwavering support throughout my academic career, for it has allowed me to, not only, become the first in my family to graduate from college, but continue furthering my education.

I would like to thank my colleagues at Flinn lab for being a fountain of knowledge, expertise, experience, and professionalism throughout my years of research there. Specifically, I would like to thank PhD student Rachel Barkey for training me on several of the lab protocols. I would like to thank PhD student Erin Doherty and undergraduate research assistants Nelly Zabala and Marie Bennett for being my blind raters for the plaque counts. Lastly, I would like to thank undergraduate research assistant David Park for assisting me in the lab during the data collection phase of this study.

TABLE OF CONTENTS

LIST OF TABLES

LIST OF FIGURES

LIST OF ABBREVIATIONS

Alzheimer's Disease ..... AD
Amyloid Precursor Protein ..... APP
Neurofibrillary Tangle ..... NFT
Metallothionein III MT3
Human Amyloid Precursor Protein Gene ..... hAPP
Human Tau Gene ..... htau
Wildtype ..... WT
Transgenic ..... Tg
Morris Water Maze ..... MWM
Parts Per Million ..... ppm
Glial Fibrillary Acidic Protein ..... GFAP
Hippocampus ..... HC
Infralimbic IL
Dentate Gyrus ..... DG
Phosphate Buffered Saline ..... PBS
Phosphate Buffered Saline with Tween ..... PBST
Zinc ..... Zn
Copper ..... Cu
Iron ..... Fe
Zinpyr-1 ..... ZP-1
Analysis of Variance ..... ANOVA
Standard Deviation ..... SD
Standard Error ..... SE
Standard Error of Mean ..... SEM
Arbitrary Fluorescence Units ..... AFU

ABSTRACT

THE NEUROPATHOLOGICAL EFFECTS OF ZINC AND COPPER SUPPLEMENTATION ON A DUAL TRANSGENIC (HAPP/HTAU) MOUSE MODEL OF ALZHEIMER'S DISEASE

Rafael Hoyos Justiniano, M.A.

George Mason University, 2022

Thesis Director: Dr. Jane M. Flinn

An imbalance of metals in the brain have shown to influence Alzheimer's Disease (AD) neuropathology and behavioral deficits both in mice and humans. Previous studies have shown that excess zinc supplementation exacerbates AD neuropathology and behavioral deficits. One reason for this could be that an excess of zinc may lead to a copper deficiency which results in neurological and behavioral problems. This study investigated the neuropathological effect of zinc+copper supplementation on a dual transgenic (hAPP/htau) mouse model of AD. Wildtype and dual transgenic mice were given regular lixit, zinc, and zinc+copper water. The relative density of AD related proteins in the brain were semi-quantified via western blotting. Amyloid and tau accumulation per brain region was assessed through histological analyses. The results of this study showed that wildtype mice showed higher levels of free zinc in the brain than the dual transgenic mice. A significant amount of this free zinc was found in hippocampal regions. Dual transgenic mice on zinc+copper water showed significantly

fewer amyloid plaques and significantly more tau tangles than dual transgenic mice on regular lixit and zinc water in specific brain regions. A significantly greater number of plaques and tangles were seen in cortical regions compared to hippocampal regions. This suggests that zinc+copper supplementation may ameliorate amyloid pathology but exacerbate tau pathology in AD mice and that zinc may bind to misfolded AD proteins resulting in less free zinc.

CHAPTER ONE: INTRODUCTION

Alzheimer's Disease (AD) is a pervasive neurodegenerative disease that is neuropathologically characterized by the accumulation of two protein fragments known as amyloid-beta and tau. Amyloid-beta is produced through the abnormal cleavage of amyloid precursor protein (APP) by secretases. The three secretases known to cleave APP are alpha, beta, and gamma secretases. Only when both beta and gamma secretases cut, is amyloid-beta produced. This abnormally large peptide then accumulates extracellularly to form neurotoxic plaques (O'Brien & Wong, 2011). Tau is a microtubule associated protein that becomes hyperphosphorylated in AD. Hyperphosphorylated tau composes intracellular neurofibrillary tangles (NFT), which are also toxic to neurons (Small & Duff, 2008).

AD is the leading cause of dementia with an estimated 6.2 million Americans over the age of 65 having the disease and is projected to increase to 13.8 million by 2060 if no new cure or ameliorating factor is presented by then. AD is the sixth leading cause of death in the United States and the fifth leading cause of death of Americans over the age of 65. Currently there is no cure for AD, with present therapies aimed at managing symptoms rather than treating a cause ("2021 Alzheimer's Disease Facts and Figures," 2021). Given the growing amount of death and suffering attributed to this disease, it has become important to understand the neural mechanisms involved with this disease to

form therapies that can prevent, stop, or reduce the accumulation of amyloid-beta and tau in a manner that safely averts or ameliorates cognitive and behavioral deficits.

Patterns of Plaque and NFT Formation

A pattern of accumulation can be seen with those who have AD. This pattern is characterized through the Braak staging system. This system includes six stages (stages I-VI) which show the relative amount of NFTs seen in brain regions throughout the progression of AD (Braak & Braak, 1991). Although imperfect, the six stages seem to closely correlate with the severity of cognitive and behavioral deficits, which demonstrates how closely related the accumulation of tau is to the clinical symptoms seen in individuals with AD (Braak & Braak, 1991; Small & Duff, 2008). A Braak staging system for amyloid pathology was also proposed (stages A-C), but the pattern of plaque aggregation was too diffuse and general to be able to correlate each stage with specific deficits. What was determined by the formation of the Braak staging system was that NFTs begin to accumulate in the hippocampus and related cortex, progressing to further limbic regions, with late stages seeing NFTs affecting most of association cortex and severe brain tissue loss most pronounced in the medial temporal lobe. Sensory and motor cortex seem to be spared until the very late stages of the disease (Braak & Braak, 1991).

The interaction of these two proteins in AD has been a topic of debate. Two main proposals are the amyloid hypothesis and the dual pathway hypothesis. The amyloid hypothesis is thought to be the classical proposal that has driven AD-related studies. This hypothesis postulates that the accumulation of amyloid-beta causes the hyperphosphorylation of tau, through direct interaction, and leads to cell death (Small &

Duff, 2008). Most clinical studies target the formation of amyloid plaques, but all attempts at a cure have failed. Most FDA approved drugs treat only symptoms of AD, with the goal being to deaccelerate the rate of cognitive decline (Kumar et al., 2014).

Alternatively, the dual pathway hypothesis suggest that the increase in amyloid-beta and tau hyperphosphorylation may not be so mutually exclusive in the more common form of AD (Small & Duff, 2008). The two forms of AD can be characterized as late-onset AD and early-onset AD, with late-onset AD being the most common (Farrer et al., 1997). Those with early-onset AD tend to develop symptoms before the age of 65 and as early as age 30, while those with late-onset AD develop symptoms after the age of 65. Early-onset AD is caused by rare genetic mutations seen on Amyloid Precursor Protein, Presenilin 1, and Presenilin 2 genes ("2021 Alzheimer's Disease Facts and Figures," 2021). Late-onset AD is thought to have a more environmental cause with age, diet, exercise, education, and other factors contributing to the risk of developing AD, but the APOE gene has been linked to AD with the APOE-e4 allele found to be one of the greatest risk factor for developing late-onset AD (Farrer et al., 1997).

The alternative proposal to the amyloid hypothesis, suggests that the increase in tau hyperphosphorylation and amyloid-beta may be linked by separate mechanisms caused by a "common upstream driver". What has also been suggested is that both hypotheses may be correct, but that the amyloid hypothesis may be true for those with early-onset AD, while the dual pathway hypothesis may occur in those with late-onset AD (Small & Duff, 2008). This would suggest that a separate approach targeting both the accumulation of amyloid-beta and the hyperphosphorylation of tau would be warranted,

given that the most common form of AD is late-onset, yet many of the drugs being investigated focus mainly on reducing amyloid-beta plaques (Small & Duff, 2008).

Role of Metals in AD

Given the lack of progress that has been made in finding a single cause of AD, there has been plenty of research and understanding that a multifaceted approach at studying AD would be logical given its effect on multiple brain regions and cognitive domains. One of the main focuses of this lab is to understand the effects of biometals on the brain and behavior, particularly in relation to AD. According to the "Metals Hypothesis of AD", among the many endogenous metals found within the body, copper (Cu), zinc (Zn), and iron (Fe) seem to be the focus of dysfunction seen in AD (Bush, 2008). An imbalance of these metals in the brain not only seem to exacerbate AD pathology seen in the brain of humans and other animals, but may also precede the accumulation of amyloid-beta plaques and tau NFTs (Bush, 2008). There is evidence to suggest that copper, zinc, and possibly iron bind to amyloid-beta and encourages accumulation into plaques. Evidence suggests that initial toxic oligomerization of soluble amyloid-beta may be due to the interactions of copper and zinc with soluble amyloid-beta$_{42}$ at cortical and hippocampal NMDA synapses (Bush, 2008). Within healthy NMDA synapses, zinc is co-released with glutamate into the synaptic cleft following successful NMDA-induced activation. Copper is then also released by the post-synaptic neuron into the synaptic cleft. Both copper and zinc can inhibit NMDA receptor response and prevent excitotoxicity caused by an excess influx of calcium into the post synaptic neuron following activation. This would also prevent further copper from being released into the

synaptic cleft. Also, in a normal synapse, amyloid-beta would be cleared by circulation into the periphery or degradation by extracellular proteases. Copper and zinc concentrations are kept low by energy dependent reuptake mechanisms and metallothionein III (MT3), which are released by astrocytes.

There is evidence to suggest that dysfunction in AD synapses occur due to decreased mitochondrial energy and MT3 concentrations. With less energy available to support reuptake mechanisms and less MT3 to remove these metals from the synaptic cleft, the extracellular copper and zinc levels rise and increase the chances of interaction between these metals and amyloid-beta. Besides inducing plaque formation, copper, along with iron, interact with amyloid-beta to form toxic hydrogen peroxide and is thought to contribute to oxidative stress on the brain. Zinc can bind to amyloid-beta and prevent the proper clearance of amyloid-beta. Apart from the consequences seen with plaque formation, the binding of zinc and copper to amyloid-beta allows the continuation of glutamate activation of the NMDA receptor and without the inhibition provided by these metals, this would allow a dangerous increase in calcium influx and increased release of copper into the synaptic cleft (Bush, 2008).

An interaction with copper and iron is also affected by AD. APP plays a major role in oxidizing Fe^{2+} to Fe^{3+} in the cortex. This oxidation allows for Fe^{3+} to be loaded into transferrin and cleared. Zinc inhibits the ferroxidase activity of APP, and this is most likely to occur in plaques where zinc, iron, and APP are present. Ceruloplasmin also has a ferroxidase function but does not load Fe^{3+} into transferrin in the neocortex and copper is needed for ceruloplasmin to oxidize Fe^{2+}. Too much zinc can also lead to a copper

deficiency. This would mean that excess zinc would decrease iron export in cortical regions through APP, and in non-cortical regions because of decreased copper (Duce et al., 2011). This would suggest maintaining optimum levels of these metals could prove effective in reducing amyloid pathology.

The interaction between metals and tau, alone, has been less looked at in humans, but has been studied in mice models. With mice that carried the human gene for tau protein (P301L), zinc supplementation not only induced behavioral deficits such as impaired spatial memory and circadian rhythm activity, but also found significantly higher NFTs in the hippocampus compared to control mice (Craven et al., 2018). Another study using a novel AD mouse model that carried the human genes for APP and tau (hAPP/htau), found that these dual transgenic (Tg) mice given zinc supplementation via drinking water showed increased behavioral deficits and significantly greater NFT pathology in the hippocampus compared to control mice (Lippi et al., 2018).

Zinc supplementation has been prevalent among modern society, given that it is used as a preventative for age-related eye problems such as cataracts and macular degeneration. Multivitamins also contain zinc, for its immune boosting abilities, but too much zinc can lead to memory deficits and overall cognitive decline (Craven et al., 2018). An excess of zinc supplementation has shown to cause copper deficiency, which has been linked to cognitive decline and neurological disease (Maret & Sandstead, 2006; Nations et al., 2008). Given the role zinc and copper play in neuromodulation of NMDA receptors, specifically in the hippocampus, it thus makes sense that memory deficits and changes in cognition are seen when there is an imbalance in these metals. Given copper's

role in iron transport, excess zinc could then indirectly lead to anemia as well. A study looking at zinc supplementation via drinking water using Sprague Dawley rats showed that rats given excess zinc showed significantly poorer performance on the Morris Water Maze (MWM) and fear conditioning, which are cognitive tests that provide quantitative measures of hippocampal dependent spatial memory and fear learning, respectively. The addition of copper to the zinc supplement resulted in improved performance on both tests that was closer to that of control rats (Railey et al., 2010).

Experimental Models

Rodents, such as mice and rats, have been one of the main animal models used for AD research, given similarities in central nervous system structures. Most of these Tg models introduce human gene mutations into the DNA of these rodents to model AD neuropathology. Some may use one or more mutations to look at different aspects of AD. For example, in the Hsiao et al. (1996) study, the first mouse model for AD was introduced. This mouse model had one copy of the human APP gene with a mutation known as the Swedish mutation. This mutation results in the increase in amyloid-beta production. Behavioral tests, such as MWM and Y maze were used to test hippocampal dependent behaviors. MWM is used to test spatial memory and learning, while Y maze is dependent on episodic and spatial memory. These Tg mice were tested over a year and the results showed that significant impairment on the MWM was seen in these mice following 10 months of age compared to age-matched controls. This impairment on MWM was also seen in Tg mice re-tested at 12-15 months of age. Brain analyses of these mice showed a significant increase in amyloid-beta in the cortex and hippocampal

structures that accompanied the behavioral deficits (Hsiao et al., 1996). This model was used to show the correlation between an increase in amyloid-beta and behavioral deficits that mimics AD in humans.

A study by Corona et al. (2010) used a 3xTg-AD mouse model, which helped illustrate the contradictory results found in studies looking at zinc and AD. Given the results, which tend to show that AD mice that are supplemented with zinc show greater AD neuropathology and behavioral deficits, this study found that zinc supplementation of 30 p.p.m. improved hippocampal-dependent memory and reduced plaques and NFTs. This study argued that this effect illustrates a specific hypothesis which postulates that an excess of zinc can exacerbated AD pathology, but a deficit of zinc can increase plaque volume in AD mice (Corona et al., 2010). While there is contradictory evidence to the effect of supplemented zinc, no study has looked at both copper and zinc supplementation on a dual (hAPP/htau) Tg mouse model.

The proposed mouse model that will be used in this current study will be the same one used in the Lippi et al. (2018) study. The Lippi et al. (2018) study used a novel hAPP/htau dual Tg mouse model that modeled both amyloid and tau pathology. This study argued that this model was superior given that more focus is being made on understanding tau pathology, all drug research that have focused solely on amyloid pathology have failed, and this has led to no new drug development for AD since the early 2000s. This study looked at the effects of zinc supplementation via drinking water on the behavior and brain pathology of dual (hAPP/htau) Tg mice and htau mice, compared to control mice. Behavior was assessed at 3.5 and 7 months of age, while the

brains were analyzed at 8 months of age. Biochemically, the study showed that the dual Tg mice showed overall greater amyloid and tau pathology in the hippocampus compared to htau and control mice, also that dual Tg mice given zinc water had greater NFTs in the hippocampus compared to htau mice on zinc water. Deficits in both cognitive and non-cognitive behaviors, like those seen in AD were also displayed by the dual Tg mice (Lippi et al., 2018).

This study used a similar experimental paradigm as the Lippi et al. (2018) study, with the addition of a copper and zinc supplement. It focused only on the neuropathology of dual Tg (hAPP/htau) mice on regular lixit, zinc, and zinc+copper water, while the behavior was assessed in another study (Gervase et al., 2021).

CHAPTER TWO: MATERIALS AND METHODS

Animals

Dual Tg mice were attained through the breeding of a cross between J20 hAPP mice (Tg(PDGFB-APPSwIND)20Lms/2Mmjax) and rTg4510 tau mice (Tg(Camk2a-tTA)1Mmay Tg(tet0-MAPT*P301L)#Kha/J) obtained through Jackson Laboratory and MMRRC. Mice without any mutations are known as wildtype (WT) mice. Animal genotype was confirmed through genetic testing via tail snips analyzed by Transnetyx, Inc.

Animal Care

Previous animal housing, feeding, and general care was taken care of by the Krasnow Institute Animal Facility staff at George Mason University. The mice were handled weekly as part of the separate behavioral study protocol and were kept on a 12-hour light/dark cycle as per the animal facilities general protocol.

Water

Wildtype and dual Tg mice were assigned into three groups of water. This included regular lixit, zinc, and zinc+copper water that was administered ad libitum. The preparation of zinc water (Craven et al., 2018; Linkous et al., 2009; Lippi et al., 2018; Railey et al., 2010) and, zinc+copper water (Railey et al., 2011) was done following previous studies' protocol on site. The mice received the water via plastic water bottles,

following 8 weeks of age, attached to their cages and the bottles were shaken regularly to ensure proper distribution of metal in the water. The water was prepared before behavioral testing. The metal content in the water was tested via coupled plasmaoptical emission spectroscopy and ion chromatography at the United States Geological Survey (USGS) in Reston, VA.

Zinc Water Preparation

The zinc water was prepared by using a 10,000-ppm solution of Zn dissolved in 10L of water. The solution was buffered using sodium carbonate and brought to a pH of approximately 7, resulting in a 10-ppm solution of zinc carbonate. The water bottles were prepared on site, labeled, and documented in accordance with previous studies (Linkous et al., 2009; Lippi et al., 2018; Railey et al., 2010, 2011).

Zinc and Copper Water Preparation

The zinc+copper water was prepared as a solution of 10-ppm zinc carbonate with the addition of 0.25-ppm copper carbonate in accordance with a prior study (Railey et al., 2011).

Brain Extraction

Twenty-four hours following the termination of the separate behavioral study, at 8 months of age, the mice were euthanized via gaseous carbon dioxide (CO2) overdose and subsequently decapitated using guillotine. The mice brains were extracted, flash frozen using dry ice, and then stored in a -80ºC freezer.

Western Blotting

Western Blotting similarly followed the Lippi et al. (2018) study protocol using a random sample of mice. The left hemisphere of the flash frozen brains was selected and homogenized in ice-cold RIPA buffer with Halt™ protease/phosphatase inhibitor cocktail (ThermoFisher) using a glass dounce tissue grinder. The homogenized samples were centrifuged at 14,000 RPM for 20 minutes at 4ºC. The soluble protein concentrations were determined using the BCA protein assay kit (Pierce™, ThermosFisher). Samples were then loaded onto NuPAGE ™ 4-12% Bis-Tris gels (Invitrogen) and transferred to nitrocellulose membranes using the IBlot 2 gel transfer device (ThermoFisher). The membranes were then blocked with 5% non-fat dried milk in PBST (1x phosphate-buffered saline with 0.1% Tween 20 (Sigma Aldrich)) for 30 min. and incubated with primary antibody overnight at 4ºC. Primary antibodies included: GAPDH (1:1000, Abcam), GFAP (1:1000, Cell Signaling), Tau-5 monoclonal antibody (1:1,000, ThermoFisher) , and Phospho-Tau (Ser202,Thr2-5) monoclonal antibody (AT8) (1:1,000 ThermoFisher). Membranes were then washed three different times in PBST, then blocked in appropriate HRP-conjugated secondary antibody (1:20,000, Abcam) for one hour. Blots were treated with SuperSignal West Pico PLUS Chemiluminescent Substrate (ThermoFisher) then imaged using the G:Box Chemi-XT4 (Syngene) system with GENESys software (V1.2.5.0). The bands were analyzed using ImageJ (NIH) software. This allowed for semi-quantification of protein per brain sample looking at tau, phosphorylated tau, and glial fibrillary acidic protein (GFAP). GFAP serves as a marker for activated astrocytes, which increase with worsening pathology (Lippi et al., 2018).

Four brains per experimental group (regular lixit, zinc, and zinc+copper) were assessed for both wildtype and dual Tg mice (N = 24).

Histology

Brains that were not used for western blotting were used for histology where coronal slices of fresh frozen brain tissue were taken using the Leica CM3050s cryostat at 16µm thickness and mounted on charged slides (SuperFrost Plus Slides, Fisher Scientific). Slices were taken of the infralimbic (IL) region and the hippocampus (HC) and stored in a -80ºC freezer to be stained, except for in the case of Zinpyr-1 staining where freshly sliced brain tissue was used as perfused brain tissue has shown to yield unreliable results (Lippi et al., 2018). Unlike with western blotting, brain analyses using histology were done on whole brain sections. A sample size of five mice per experimental group was used for each stain performed, except for Congo-Red and Thioflavin-S, because wildtype mice do not have any mutations and thus would not produce any visible plaque or NFT pathology. Total sample size per group is shown in Table 1 for the entirety of this study.

Table 1: Sample Size Per Group for Tissue Analysis
Brain analyses include Western Blotting (WB), Zinpyr-1 (ZP-1), Congo-Red (CR), and Thioflavin-S (TS) staining. N/A= not applicable.

Brain Analyses	Dual Tg	Wildtype
Regular Lixit Water		
WB	4	4
ZP-1	5	5
CR	5	N/A
TS	5	N/A
Zinc Water		
WB	4	4
ZP-1	5	5
CR	5	N/A
TS	5	N/A
Zinc+Copper Water		
WB	4	4
ZP-1	5	5
CR	5	N/A
TS	5	N/A

Zinpyr-1 (ZP-1)

Zinpyr-1 was used to stain for free zinc using fluorescence and followed the protocol used in the Lippi et al. (2018) study. Given the light-sensitivity of this stain, the following procedure was done under minimal light conditions. A 1mM stock solution of Zinpyr-1 (Abcam, ab145349) was prepared in DMSO followed by a 17µM working solution made using 0.9% sodium chloride solution. Infralimbic and hippocampal slices on charged slides were immediately covered in working solution (enough to cover section) for 2-3 minutes in darkness then after were tilted to remove the ZP-1 solution. Working solution was made fresh each day of use. Following the 2-3 minutes, slices were immediately imaged using an Olympus BX51 fluorescence microscope with a fluorescein isothiocyanate (FITC) cube and mercury burner. Slices were imaged at 2x objective with

consistent exposure time between each sample. Images were analyzed using ImageJ (NIH) software. Images were semi-quantified by subtracting the background then measuring five separate areas, which showed fluorescence within the brain region of interest, to obtain the average fluorescence values in each region. Average fluorescence values were collected for the infralimbic region, dentate gyrus (DG), CA3, and CA1 regions of the hippocampus. Higher fluorescence values were indicative of higher amounts of free zinc.

HT-60 Congo-Red Staining

Amyloid plaques were visualized using the HT-60 Congo Red Staining Kit following the manufacturer's instructions (Sigma Aldrich). Tissue slides from dual Tg samples were soaked in Mayer's hematoxylin solution for 2 minutes, then rinsed in distilled water for 5 minutes. Then the slides were soaked in alkaline sodium chloride solution for 20 minutes followed by soaking in Congo Red solution for 30 minutes. Finally, the slides were rinsed in ethanol before being cleared in xylene for 3 minutes and coverslipped with DPX. Slides were left to dry overnight before imaging. After drying, images were taken using an Olympus BX51 microscope at 20x objective with consistent exposure time between samples. The images were shown to 3 blind (to the experimental conditions) raters, who assessed the overall plaque count. Their counts were averaged together and used for subsequent statistical analysis.

Thioflavin-S staining

NFTs were visualized using a previously modified thioflavin-S staining protocol which uses fluorescence to stain for NFTs (Craven et al., 2018; Lippi et al., 2018; Sun et

al., 2002). Tissue slides from dual Tg samples were let to come to room temperature if being taken directly from a -80ºC freezer. The room lights were then turned off as this stain was light sensitive. Afterwards, the slides were placed in paraformaldehyde (PFA) for 8 minutes. Then they were placed in 0.25% potassium permanganate for 4 minutes followed by 1% sodium borohydride for 4 minutes and subsequently rinsed in distilled water. The slides were then placed in 0.05% Thioflavin-S (Sigma Aldrich) prepared in 50% ethanol for 8 minutes followed by two different placements in 80% ethanol for 10 seconds each, then 3 different rinses in distilled water. Finally, the slides were placed in 10x PBS in the fridge for 30 minutes and subsequently rinsed in distilled water. Slides were immediately imaged using an Olympus BX51 fluorescence microscope with a FITC cube and mercury burner under a 20x objective with a consistent exposure time between slides. Images were analyzed using ImageJ (NIH) software. Each image's color threshold was adjusted via the default setting with the analysis of particles adjusted to 100 pixels across all images.

Statistical Analysis

All values for the statistical analysis are presented as mean ± *SEM*. Two-way ANOVAs, with genotype and water as independent variables, were run for the dependent variable measured in western blotting. A 2 (genotype) x 3 (water) x 4 (brain region) mixed ANOVA was run for the ZP-1 fluorescence values used to measure free zinc. 3 (water) x 6 (brain region) mixed ANOVAs were run for Thioflavin-S and Congo Red, with NFTs and plaques as their dependent variables respectively. The brain regions analyzed via histology included the infralimbic region, and the DG, CA3, and CA1

regions of the hippocampus. While analyzing for plaques and NFTs via Congo Red and Thioflavin-S staining, these pathologies were also seen in cortex surrounding the hippocampus, so in addition to the infralimbic and hippocampal regions, the cortex surrounding the hippocampus (denoted as cortex above and lateral cortex) was added as two brain regions analyzed for these two stains. Zinpyr-1 stain did not show any fluorescence for the cortex surrounding the hippocampus, so the two brain regions were not included in the analysis for this stain. The brain regions analyzed are described in Figures 1 and 2. All the data was analyzed using the statistical package SPSS v. 21, with significance considered reached at $p < .05$. Significant main effects were followed up by Bonferroni post-hoc analysis. Greenhouse-Geisser corrections were used in cases where sphericity could not be assumed in mixed ANOVA analyses.

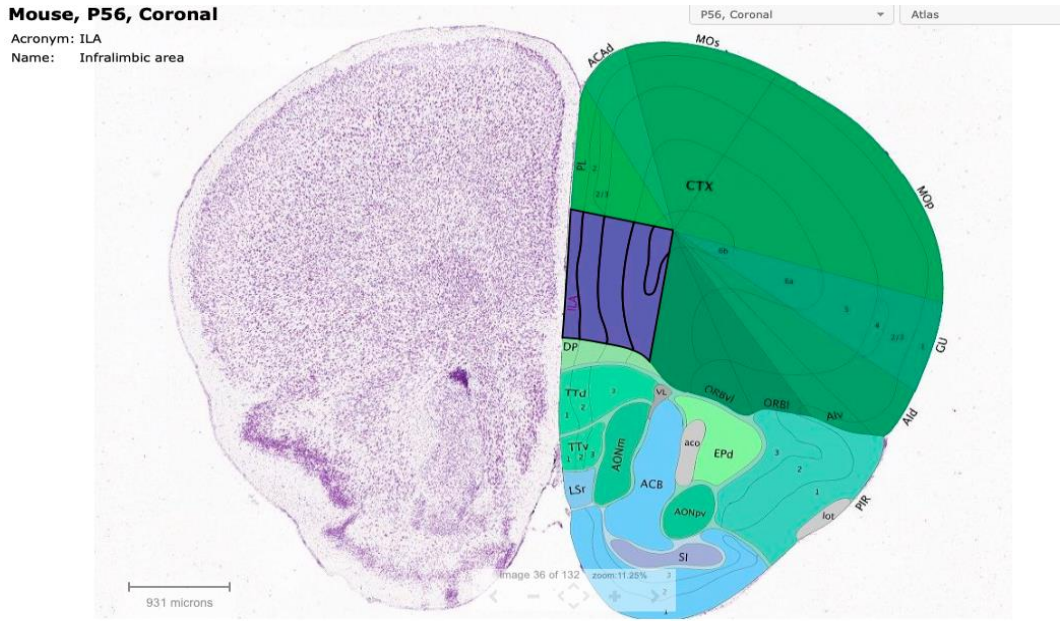

Figure 1: Coronal Section of Infralimbic Area

The Infralimbic region was one brain region analyzed for Zinpyr-1, Thioflavin-S, and Congo Red. Shown here as ILA in purple (Allen Institute for Brain Science, 2004).

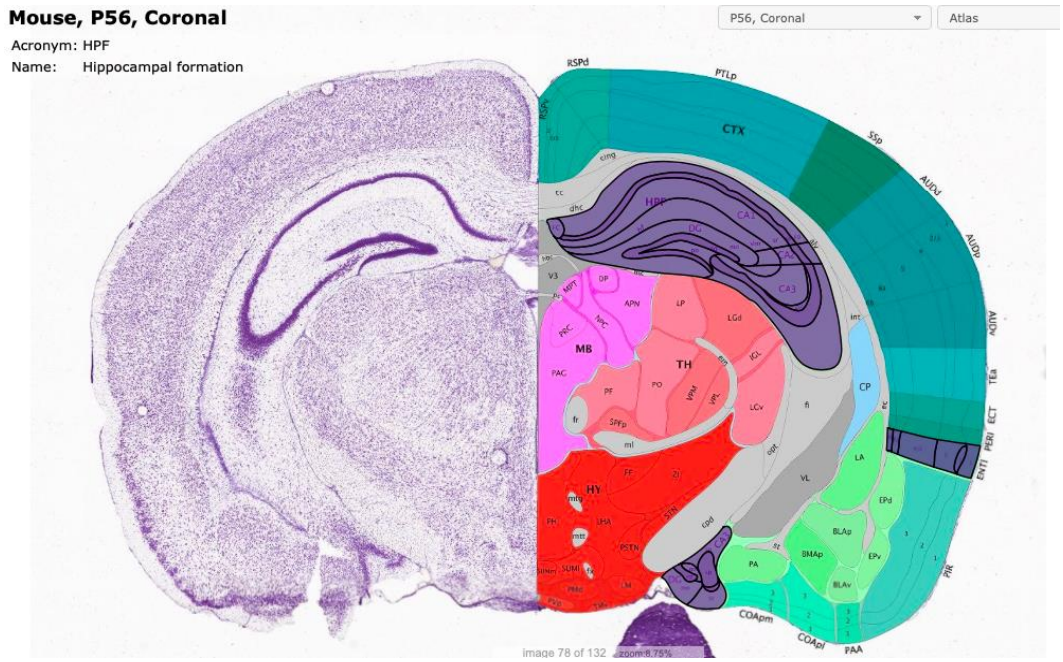

Figure 2: Coronal Section of Hippocampus

Brain regions analyzed for Zinpyr-1, Congo Red, and Thioflavin-S also included the DG, CA3, and CA1 regions of the hippocampus shown in purple. The cortex above the hippocampus as well as the lateral cortex were additionally included in the analysis for Congo Red and Thioflavin-S. The cortex above the hippocampus was defined in this study as including the retrosplenial area (RSPv and RSPd), posterior

parietal association areas (PTLp), and primary somatosensory area (SSp). The lateral cortex was defined in this study as including the auditory areas (AUDd, AUDp, AUDv), temporal association areas (TEa), ectorhinal area (ECT), perirhinal area (PERI), and entorhinal area (ENTI) (Allen Institute for Brain Science, 2004).

CHAPTER THREE: RESULTS

Western Blotting

GFAP

A 2x3 ANOVA was performed to analyze the effect of genotype (dual Tg and WT) and water (regular lixit, zinc, and zinc+copper) on the adjusted relative density of GFAP. GAPDH was used as the loading control (Figure 3). Analysis of GFAP band density values showed a significant effect of genotype, $F(1,18) = 49.647$, $p < .001$, where dual Tg mice showed significantly higher GFAP than wildtype mice (Figure 4). There showed no significant effect of water, $F(2,18) = .011$, $p = .989$, or interaction between genotype and water, $F(2,18) = .811$, $p = .460$ (Figure 5).

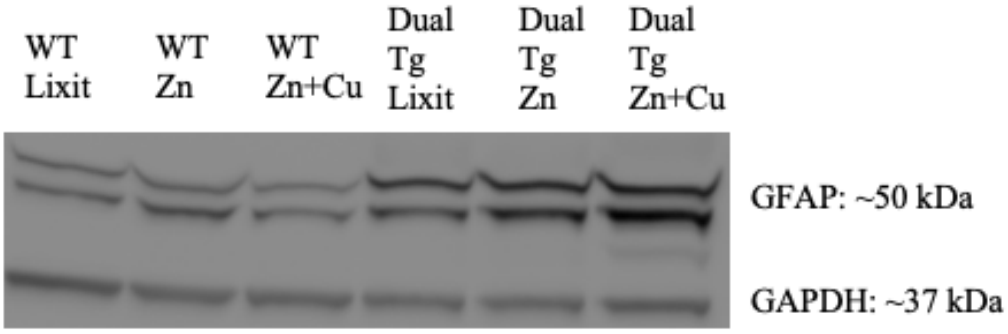

Figure 3: Representative GFAP Western Blot
A representative GFAP western blot shows the bands for GFAP and GAPDH (loading control). Each lane is indicative of a sample brain within the experimental group labeled at the top. The approximate molecular weight for each protein is shown on the right.

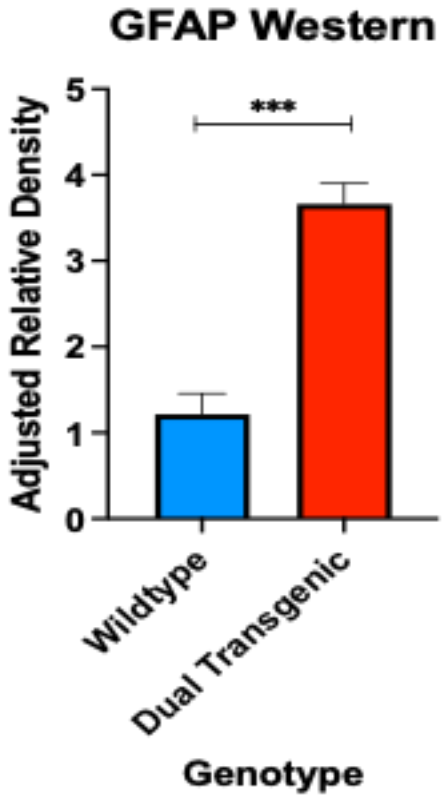

Figure 4: GFAP Genotype Difference

Figure 4 shows the adjusted relative density of GFAP for dual Tg and wildtype mice. Dual Tg mice ($\bar{X}$= 3.66, *SD* = 1.07) showed significantly higher GFAP than wildtype mice ($\bar{X}$= 1.21, *SD* = 0.37). Error bars indicate ± *SEM*. *** indicates $p \leq .001$.

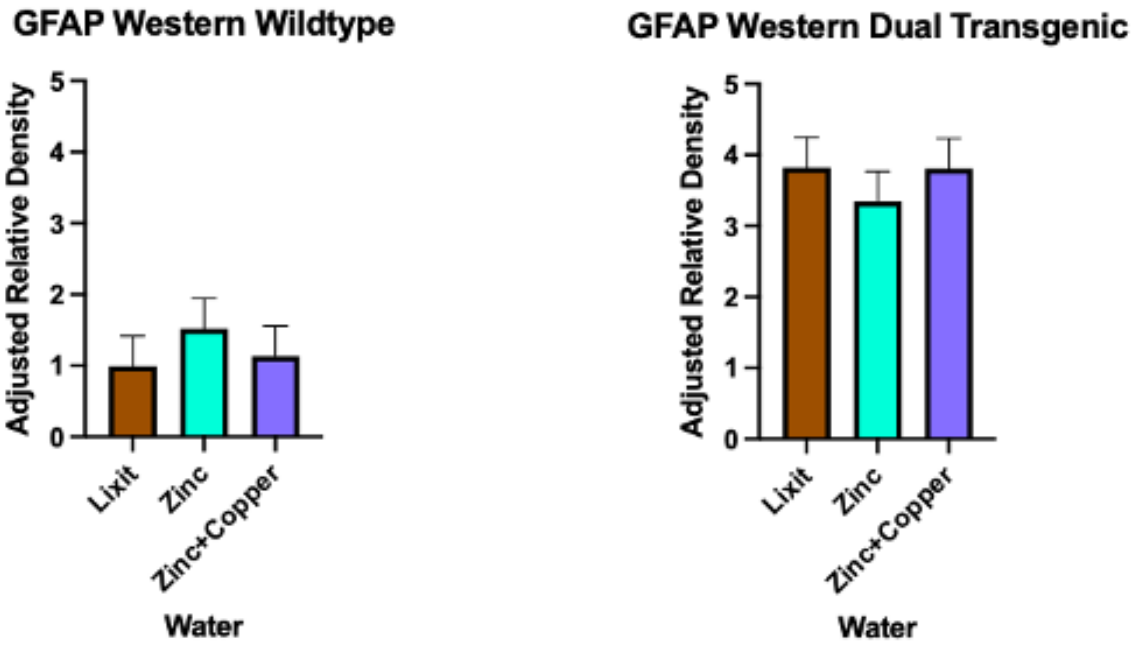

Figure 5: GFAP Water Differences
Left figure shows the adjusted relative density of GFAP for the wildtype mice on regular lixit ($\bar{X}$= 0.99, *SD* = 0.41), zinc ($\bar{X}$= 1.52, *SD* = 0.31), and zinc+copper ($\bar{X}$= 1.13, *SD* = 0.21) water. Right figure shows the relative GFAP density for the dual Tg mice on regular lixit ($\bar{X}$= 3.82, *SD* = 0.99), zinc ($\bar{X}$= 3.34, *SD* = 1.60) and zinc+copper ($\bar{X}$= 3.80, *SD* = 0.69) water. No significant water effects or interaction between genotype and water were seen. Error bars indicate ± *SEM*.

Phosphorylated Tau

A one-way ANOVA was performed to compare the effect of water (regular lixit, zinc, and zinc+copper) on the adjusted relative density of phosphorylated tau. Dual Tg mice were the only mice of interest, given that they had the htau mutation. Wildtype mice did not show any bands for phosphorylated tau. GAPDH was used as a loading control (Figure 6). There showed no significant effect of water on the adjusted relative density of phosphorylated tau, $F(2,9) = .592$, $p = .573$ (Figure 7).

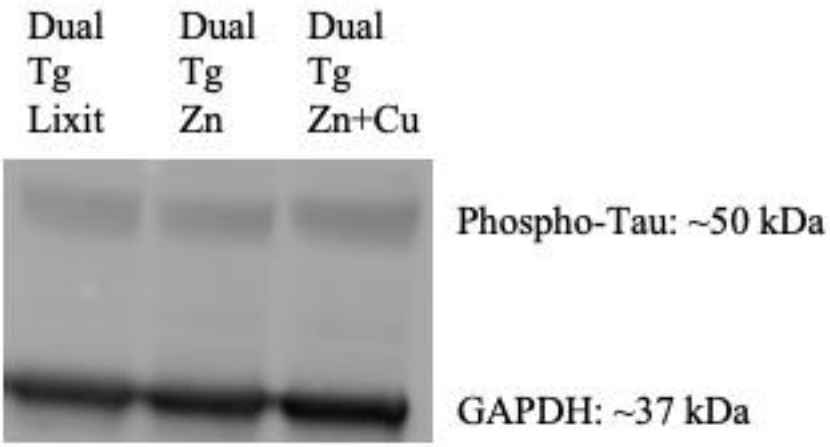

Figure 6: Representative Phosphorylated Tau Western Blot
A representative phosphorylated tau western blot shows the bands for phosphorylated tau (Phospho-Tau) and GAPDH (loading control). Each lane is indicative of a sample brain within the experimental group labeled at the top. The approximate molecular weight for each protein is shown on the right.

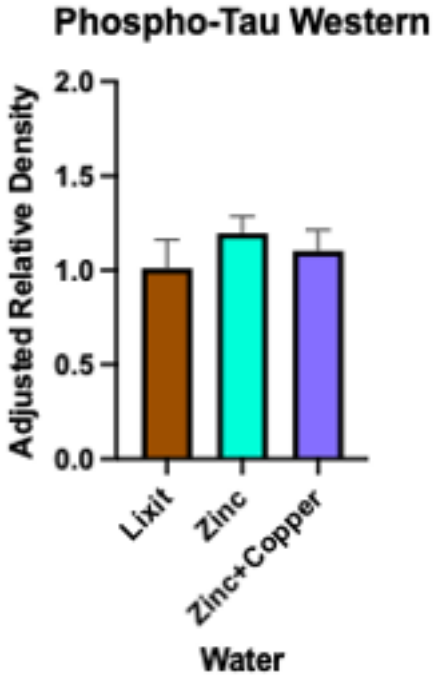

Figure 7: Phosphorylated Tau Water Differences
Figure 7 shows the adjusted relative density of phosphorylated tau (Phospho-Tau) for the dual Tg mice on regular lixit ($\bar{X}$= 1.01, *SD* = 0.15), zinc ($\bar{X}$= 1.19, *SD* = 0.18), and zinc+copper ($\bar{X}$= 1.10, *SD* = 0.22) water. There showed no significant water effect. Error bars indicate ± *SEM*.

Total Tau

A one-way ANOVA was performed to compare the effect of water (regular lixit, zinc, and zinc+copper) on the adjusted relative density of total tau (Tau-5). Dual Tg mice were the only mice of interest, given that they had the htau mutation. Wildtype mice did not show any bands for total tau. GAPDH was used as a loading control (Figure 8). There showed no significant effect of water on the adjusted relative density of total tau, $F(2,9) = 1.701$, $p = .236$ (Figure 9).

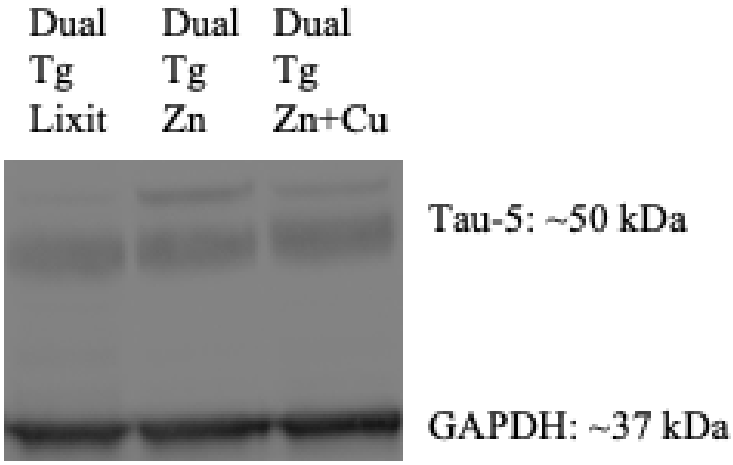

Figure 8: Representative Total Tau Western Blot
A representative total tau western blot shows the bands for total tau (Tau-5) and GAPDH (loading control). Each lane is indicative of a sample brain within the experimental group labeled at the top. The approximate molecular weight for each protein is shown on the right.

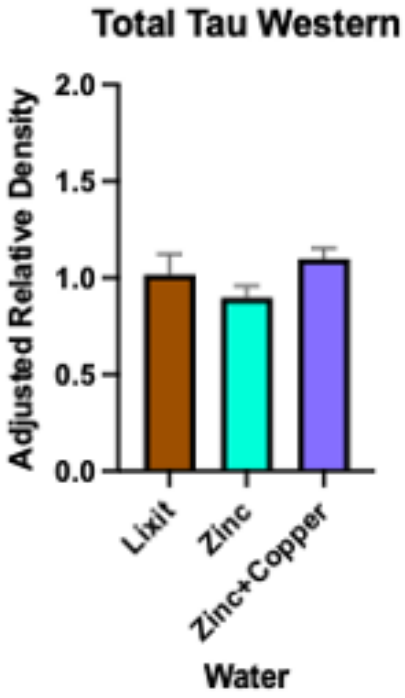

Figure 9: Total Tau Water Differences
Figure 9 shows the adjusted relative density of total tau (Tau-5) for the dual Tg mice on regular lixit ($\bar{X}$= 1.02, *SD* = 0.21), zinc ($\bar{X}$= 0.90, *SD*= 0.12), and zinc+copper ($\bar{X}$= 1.10, *SD* = 0.11) water. There showed no significant water effect. Error bars indicate ± *SEM*.

Phosphorylated Tau/Total Tau Ratio

The ratio of phosphorylated tau and total tau was calculated for each sample and used to perform a one-way ANOVA to compare the effect of water (regular lixit, zinc, and zinc+copper) on phosphorylated tau expression relative to total tau expression. There showed no significant effect of water on the ratio of phosphorylated tau/ total tau $F(2,9) = 2.350$, $p = .151$ (Figure 10).

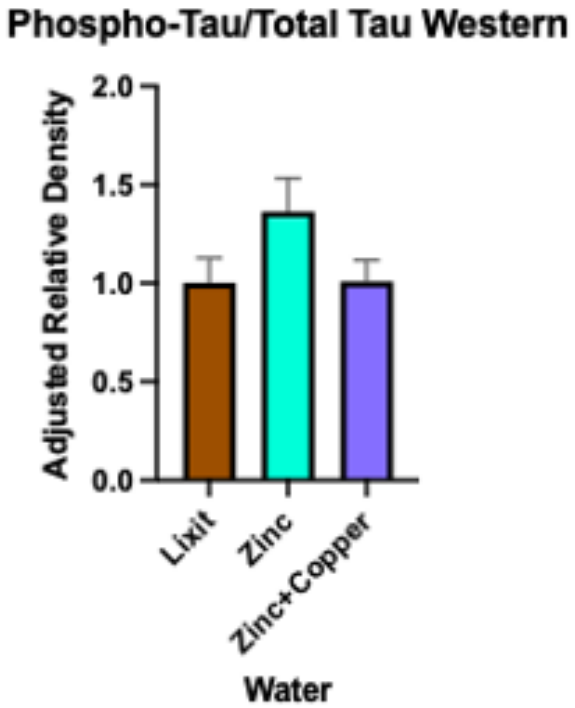

Figure 10: Phosphorylated Tau/Total Tau Ratio Water Differences
Figure 10 shows the ratio of phosphorylated tau (Phospho-Tau) and total tau (Tau-5) for the dual Tg mice on regular lixit ($\bar{X}$= 1.00, *SD* = 0.25), zinc ($\bar{X}$= 1.36, *SD*= 0.33), and zinc+copper ($\bar{X}$= 1.01, *SD* = 0.21) water. There showed no significant water effect. Error bars indicate ± *SEM*.

Histology

Zinpyr-1

A 2 (genotype) x 3 (water) x 4 (brain region) mixed ANOVA was run for Zinpyr-1 fluorescence values used to measure free zinc. Hippocampal (DG, CA3, and CA1) and infralimbic (IL) brain regions were used as repeated measures (Figure 11). Significant main effects of brain region, $F(3,72) = 80.46$, $p < .001$, and genotype, $F(1,24) = 4.678$, $p = .041$ were detected. Wildtype mice showed significantly greater free zinc than the dual Tg mice (Figure 12). Simple effects analysis revealed that the DG showed significantly greater free zinc than the CA3 ($p < .001$), CA1 ($p < .001$) and IL ($p < .001$) regions. The

IL region also showed significantly less free zinc than the CA3 ($p < .001$) and CA1 ($p = .004$) (Figure 13). There showed no significant interaction effect. Although a slight trend difference was seen where the dual Tg mice on zinc showed higher free zinc than the dual Tg mice on zinc+copper water ($p = 0.086$) (Figure 14).

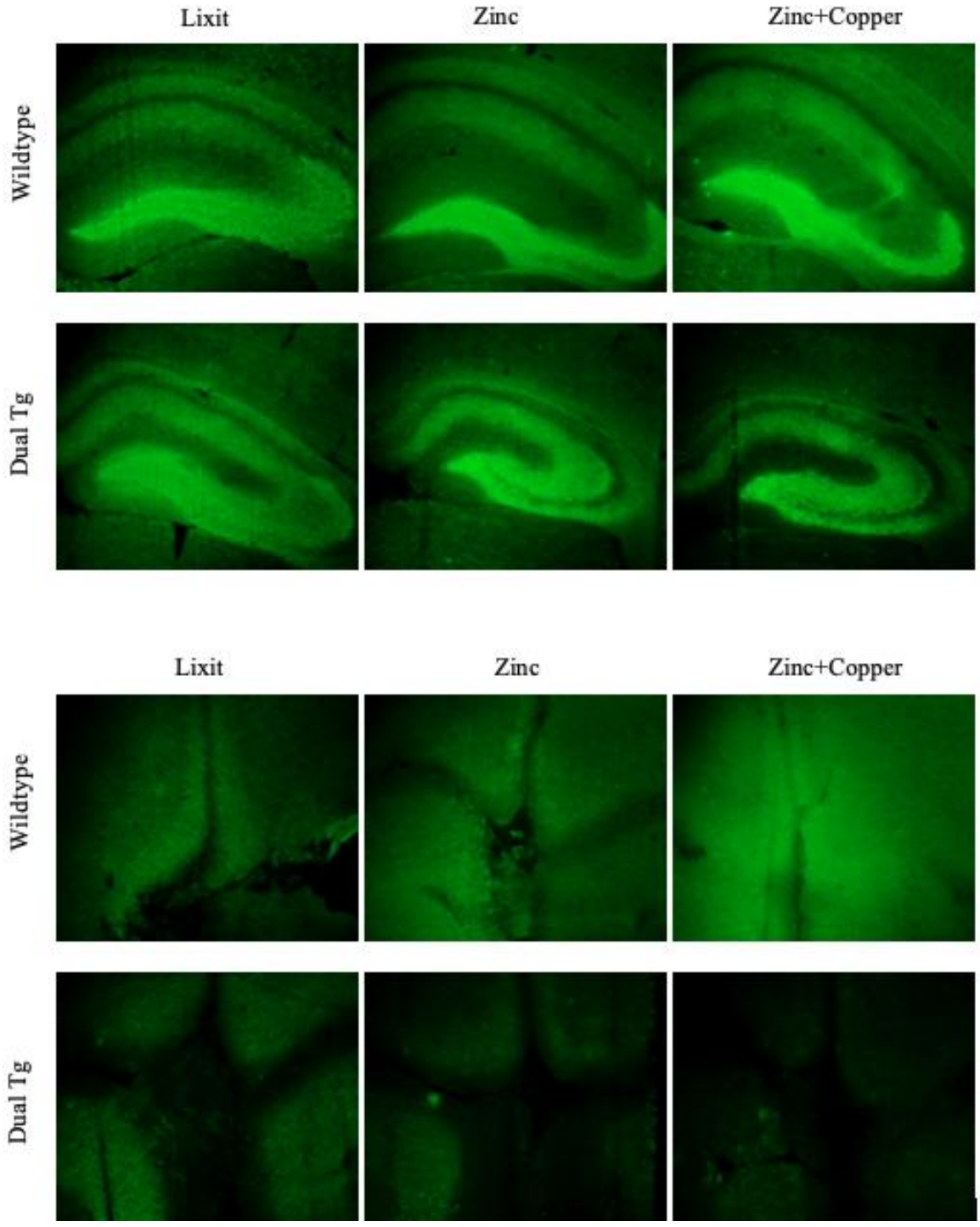

Figure 11: Representative Zinpyr-1 Stains for Free Zinc
Figure 11 shows representative zinpyr-1 stains of the hippocampal (top two rows) and infralimbic (bottom two rows) coronal slices. The labels on top of the images indicate the water the mice were on and the labels to the left indicate the genotype of the sample. Greater fluorescence is indicative of greater free zinc present.

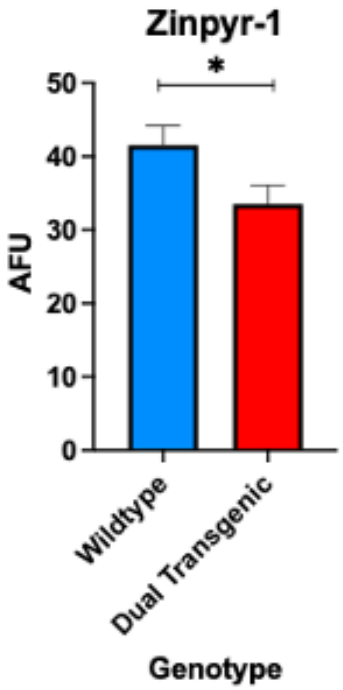

Figure 12: Zinpyr-1 Genotype Difference
Figure 12 shows the amount of free zinc measured in arbitrary fluorescence units (AFU) for dual Tg ($\bar{X}$= 33.51, *SE* = 2.63) and wildtype mice ($\bar{X}$= 41.55, *SE* = 2.63). Wildtype mice showed significantly higher free zinc than dual Tg mice (p = .041). Error bars indicate ± *SEM*. * indicates $p < .05$.

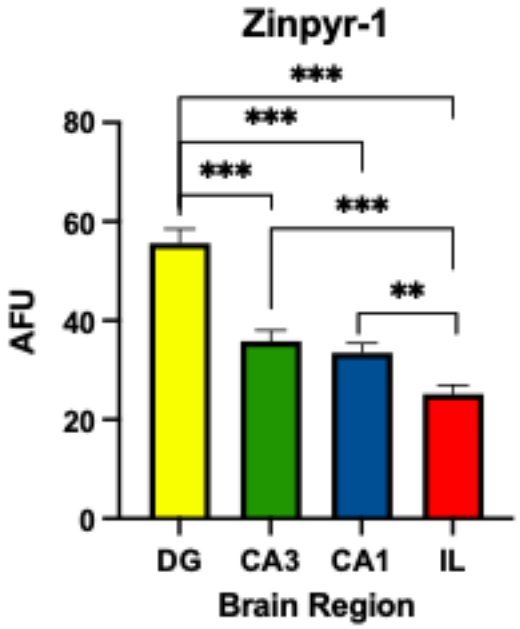

Figure 13: Zinpyr-1 Brain Region Differences

Figure 13 shows the amount of free zinc measured in arbitrary fluorescence units (AFU) for each brain region. There showed a main effect of brain region ($p < .001$). The DG ($\bar{X} = 55.62$, $SE = 2.86$) showed significantly greater free zinc than CA3 ($\bar{X} = 35.83$, $SE = 2.23$, $p < .001$), CA1 ($\bar{X} = 33.49$, $SE = 1.95$, $p < .001$) and IL ($\bar{X} = 25.19$, $SE = 1.75$, $p < .001$) regions. The IL region also showed significantly less zinc than CA3 ($p < .001$) and CA1 ($p = .004$). Error bars indicate ± *SEM*. * indicates $p < .05$, ** indicates $p \leq .01$, and *** indicates $p \leq .001$.

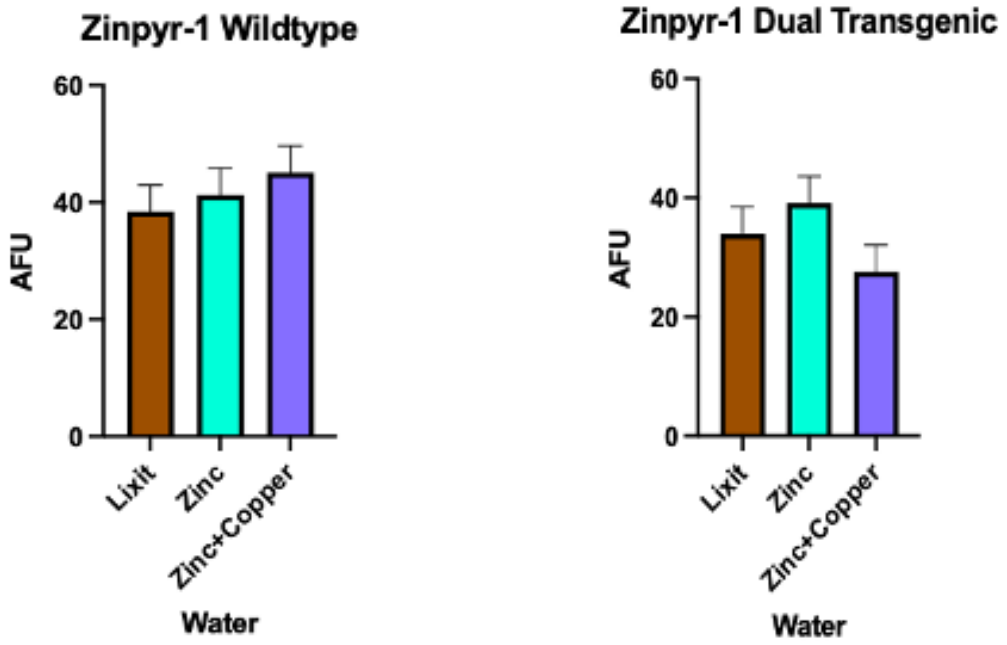

Figure 14: Zinpyr-1 Water Differences
Left figure shows the amount of free zinc measured in arbitrary fluorescence units (AFU) for the wildtype mice on regular lixit ($\bar{X}$= 38.33, *SE* = 4.55), zinc ($\bar{X}$= 41.27, *SE* = 4.55), and zinc+copper ($\bar{X}$= 45.06, *SE* = 4.55) water. Right figure shows the amount of free zinc shown for the dual Tg mice on regular lixit ($\bar{X}$= 33.91, *SE* = 4.55), zinc ($\bar{X}$= 39.08, *SE* = 4.55) and zinc+copper ($\bar{X}$= 27.53, *SE* = 4.55) water. No significant water effects or interaction between genotype and water were seen. A slight trend difference showed that the dual Tg mice on zinc had greater free zinc than the dual Tg mice on zinc+copper (p = .086). Error bars indicate ± *SEM*.

HT-60 Congo Red Staining

A 3x6 mixed ANOVA was run to analyze the effect of water (regular lixit, zinc, and zinc+copper) and brain region (DG, CA3, CA1, cortex above hippocampus, lateral cortex, and IL) on amyloid plaque expression. Only dual Tg mice were of interest given that they had the hAPP mutation (Figure 15). Three blind (to the experimental conditions) raters were shown images of HT-60 Congo Red stained plaques to familiarize themselves to the shape and color of a standard amyloid plaque. Then they were given the whole set of experimental images of plaques found in the six brain regions of interest and were

asked to count the number of plaques per brain region and make note of it. The raters were not aware of each other's plaque counts. The average number of plaques for each brain region per sample was calculated for each rater. Rater 1 showed an average of 3.16 plaques, rater 2 showed an average of 3.98 plaques, and rater 3 showed an average of 3.70 plaques for each brain region per sample. The total plaque count per brain region was averaged among the three raters and used for statistical analysis.

The mixed ANOVA revealed a significant main effect of brain region, $F(1.784, 21.402) = 10.70$, $p < .001$. There also showed a trending difference of water, $F(2,12) = 3.74$, $p = .055$. Simple effects analysis was performed and showed a trending difference between dual Tg mice on zinc and zinc+copper, with those on zinc+copper showing less plaques than those on zinc water ($p = .079$) (Figure 16). Follow up analysis of the brain region effect revealed that the cortex above the hippocampus showed significantly greater plaques than the DG ($p = .038$), CA3 ($p = .020$), and CA1 ($p = .007$). The IL region showed significantly greater plaques than CA1 ($p = .045$) (Figure 17). Dual Tg mice on different types of water showed significant differences in the number of plaques within specific brain regions. For example, dual Tg mice on zinc+copper water showed significantly less plaques in their CA3 ($p = .030$), CA1 ($p = .027$), Cortex above HC ($p = .045$), and lateral cortex ($p = .040$) than dual Tg mice on regular lixit water. Dual Tg mice on zinc+copper also showed significantly less plaques in their lateral cortex ($p = .042$) and IL ($p = .037$) region than dual Tg mice on zinc water (Figure 18).

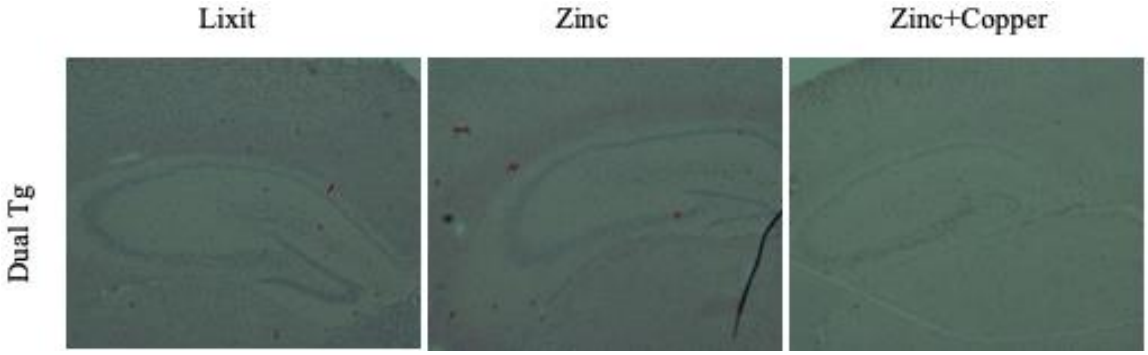

Figure 15: Representative HT-60 Congo Red Stains for Amyloid Plaques
Figure 15 shows representative HT-60 Congo Red stains of hippocampal coronal slices for dual Tg samples on regular lixit, zinc, and zinc+copper water. Amyloid plaques show bright red. Images shown were taken at 4x objective, but images that were analyzed (not shown) were taken at 20x objective.

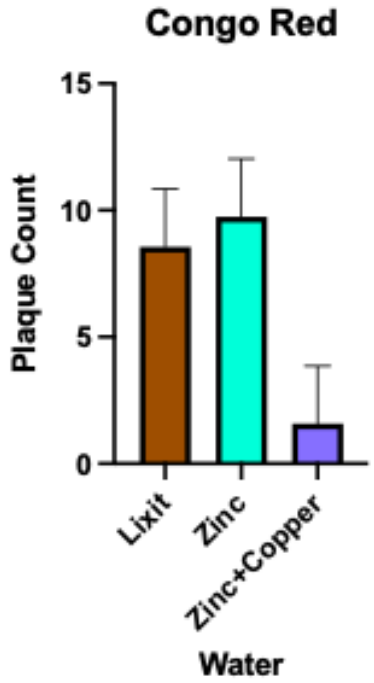

Figure 16: HT-60 Congo Red Water Differences
Figure 16 shows the differences in plaque count for dual Tg mice on regular lixit ($\bar{X}$= 8.56, *SE* = 2.28), zinc ($\bar{X}$= 9.74, *SE* = 2.28), and zinc+copper ($\bar{X}$= 1.58, *SE* = 2.28). A trending difference revealed that dual Tg mice on zinc+copper showed less plaques than dual Tg mice on zinc (p = .079). Error bars indicate ± *SEM*.

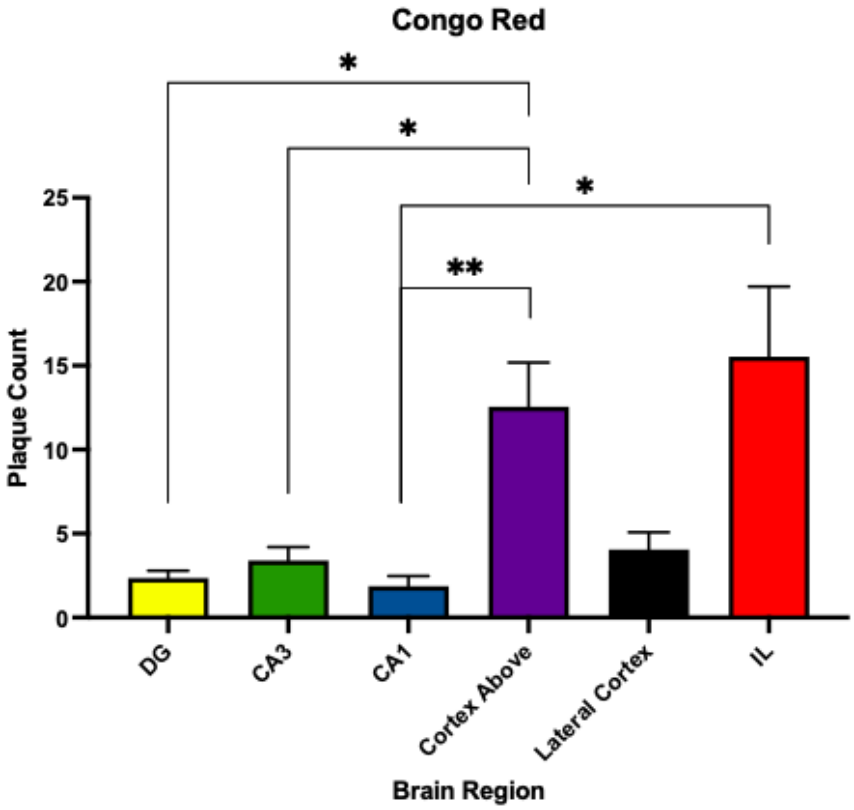

Figure 17: HT-60 Congo Red Brain Region Differences

Figure 17 shows the differences in plaque count for the brain regions of interest for dual Tg mice which include the DG ($\bar{X}$= 2.36, *SE* =0.43), CA3 ($\bar{X}$= 3.40, *SE* =0.80), CA1 ($\bar{X}$= 1.87, *SE* = 0.61), cortex above HC ($\bar{X}$= 12.56, *SE* = 2.63), lateral cortex ($\bar{X}$= 4.04, *SE* =1.03) and IL ($\bar{X}$= 15.53, *SE* = 4.17). The cortex above HC showed significantly greater plaques than the DG (p = .038), CA3 (p = .020), and CA1 (p = .007). The IL region showed significantly greater plaques than CA1 (p = .045). Error bars indicate ± *SEM*. * indicates $p < .05$ and ** indicates $p \leq .01$.

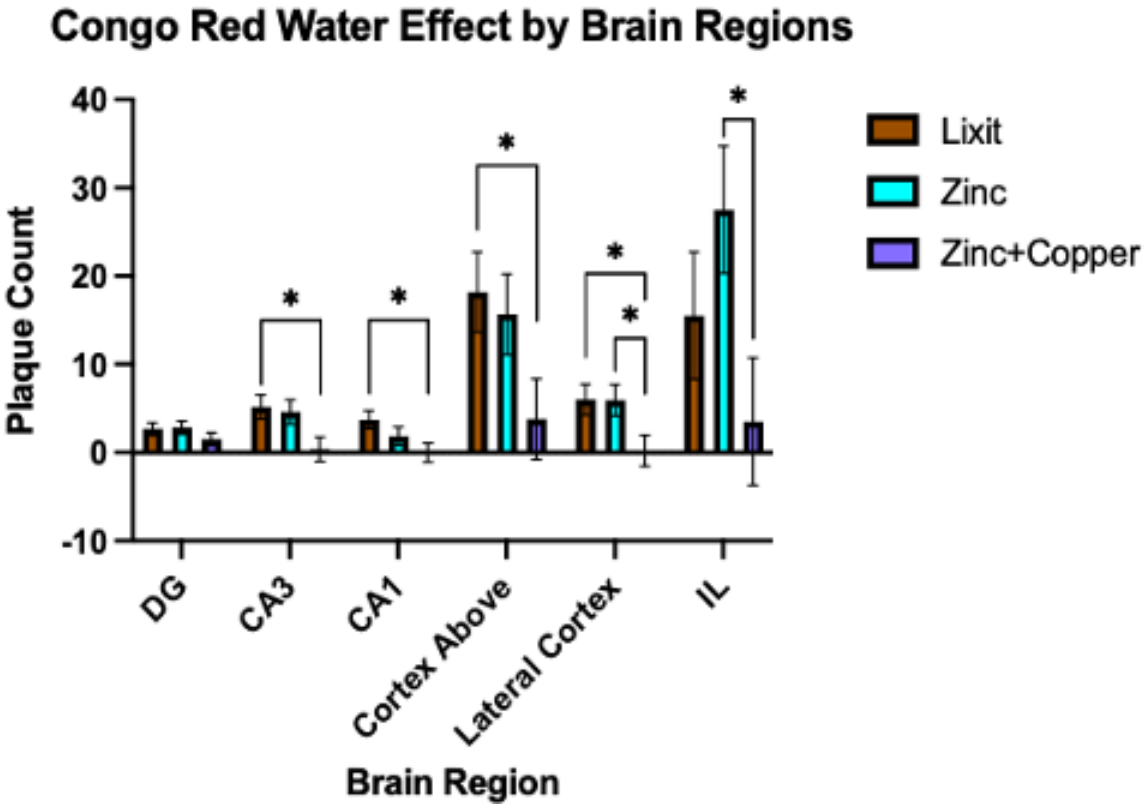

Figure 18: HT-60 Congo Red Water Effect by Brain Region
Figure 18 shows the differences in plaque count for dual Tg mice on regular lixit, zinc, and zinc+copper water by brain region. Dual Tg mice on zinc+copper water showed significantly less plaques in their CA3 (p = .030), CA1 (p = .027), cortex above HC (p = .045), and lateral cortex (p = .040) than dual Tg mice on regular lixit water. Dual Tg mice on zinc+copper also showed significantly less plaques in their lateral cortex (p = .042) and IL (p = .037) region than dual Tg mice on zinc water. Error bars indicate ± *SEM*. * indicates $p < .05$.

Thioflavin-S Staining

A 3x6 mixed ANOVA was performed to analyze the effect of water (regular lixit, zinc, and zinc+copper) and brain region (DG, CA3, CA1, cortex above hippocampus, lateral cortex, and IL) on NFT expression. Only dual Tg mice were of interest given that they had the htau mutation (Figure 19). The mixed ANOVA revealed a significant main effect of brain region, $F(2.78, 33.30) = 28.40$, $p < .001$. No significant main effect of water or significant interaction was detected (Figure 20).

Simple effects analysis was performed for the brain region main effect and showed that the DG showed the least amount of NFTs with a significantly lower tangle count than CA3 ($p = .003$), CA1 ($p < .001$), cortex above hippocampus ($p < .001$), lateral cortex ($p < .001$), and IL ($p < .001$) region. The cortex above hippocampus showed the greatest amount of NFTs with a significantly higher tangle count than CA3 ($p = .032$), CA1 ($p < .001$), IL ($p < .001$) region, and DG. The lateral cortex showed significantly greater NFTs than CA3 ($p = .012$), CA1 ($p = .004$), IL region ($p = .024$), and DG (Figure 21). Dual Tg mice on different types of water showed significant differences in the number of NFTs within specific brain regions. For example, dual Tg mice on zinc+copper water showed a significantly higher tangle count than dual Tg mice on regular lixit ($p = .019$) and zinc ($p = .025$) water in their DG. Dual Tg mice on zinc+copper water also showed a significantly higher tangle count than dual Tg mice on regular lixit ($p = .022$) and zinc ($p = .033$) water in their cortex above hippocampus. Graphically, dual Tg mice on zinc+copper had higher tangle counts in their CA3, lateral cortex, and IL as well, but was not statistically significant ($p > .05$) (Figure 22).

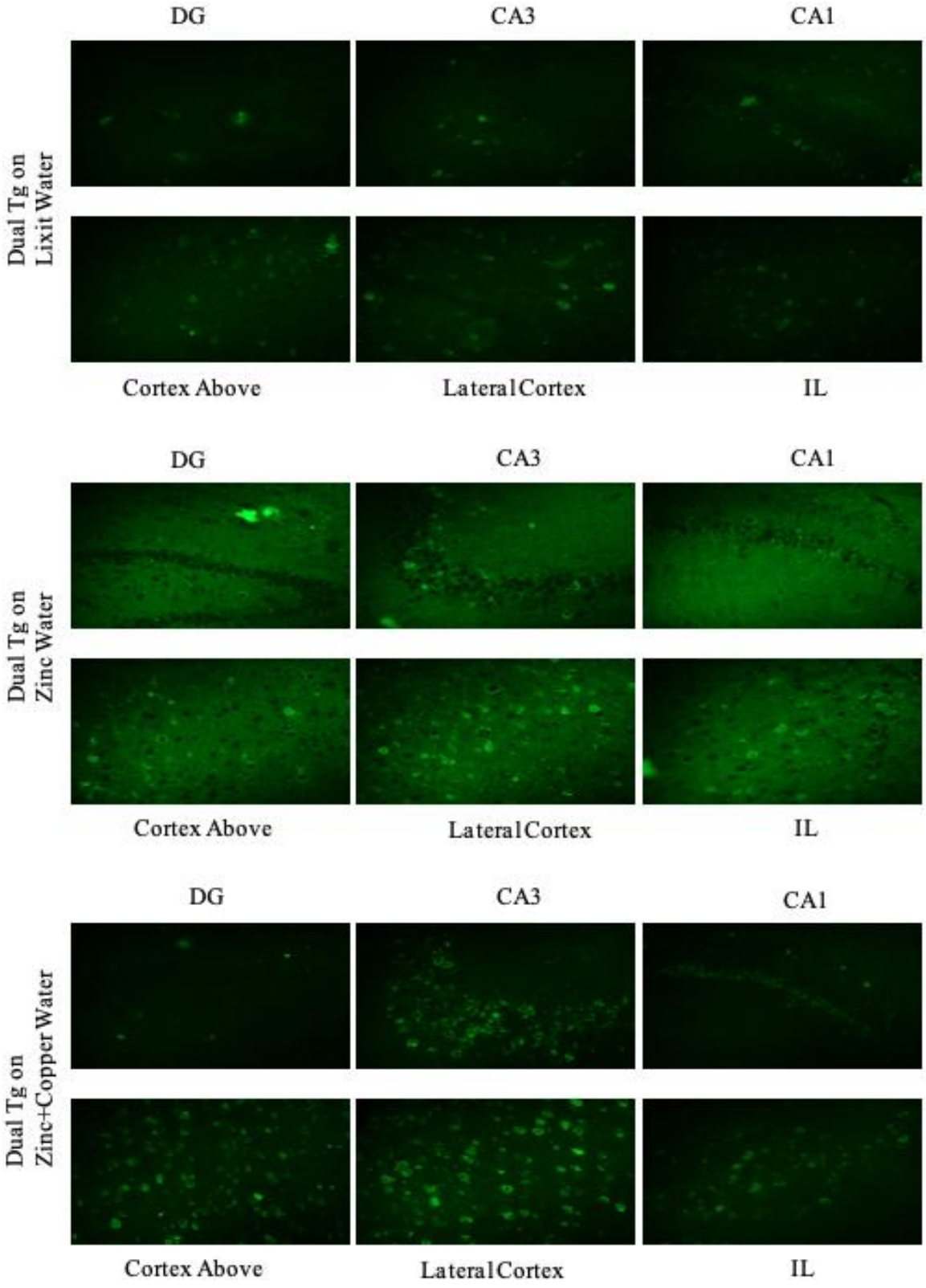
DG
CA3
CA1
Dual Tg on Lixit Water
Cortex Above
Lateral Cortex
IL
DG
CA3
CA1
Dual Tg on Zinc Water
Cortex Above
Lateral Cortex
IL
DG
CA3
CA1
Dual Tg on Zinc+Copper Water
Cortex Above
Lateral Cortex
IL

Figure 19: Representative Thioflavin S Stains for NFTs
Figure 19 shows representative Thioflavin S stains of hippocampal (DG, CA3, CA1, cortex above HC, and lateral cortex) and infralimbic coronal slices for dual Tg samples on regular lixit, zinc, and zinc+copper water. NFTs are fluorescent and bright green in this stain. Images were taken at 20x objective.

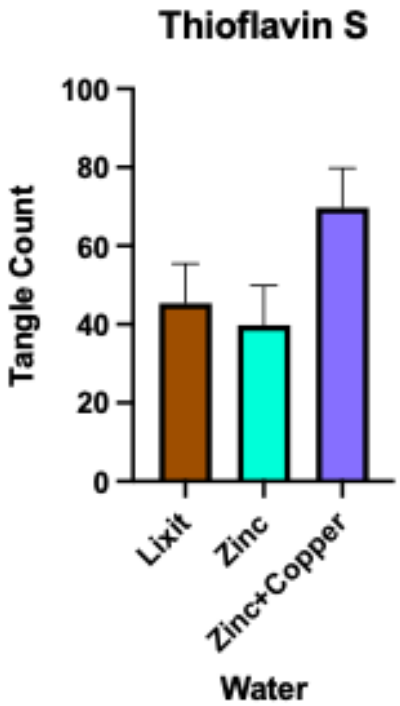

Figure 20: Thioflavin S Water Differences
Figure 20 shows the differences in tangle count for dual Tg mice on regular lixit ($\bar{X}$= 45.40, *SE* = 10.07), zinc ($\bar{X}$= 39.77, *SE* = 10.07), and zinc+copper ($\bar{X}$= 69.70, *SE* = 10.07). Although dual Tg mice on zinc+copper water showed to have a higher tangle count than dual Tg on zinc water, it was not statistically significant (*p* = .172). Error bars indicate ± *SEM*.

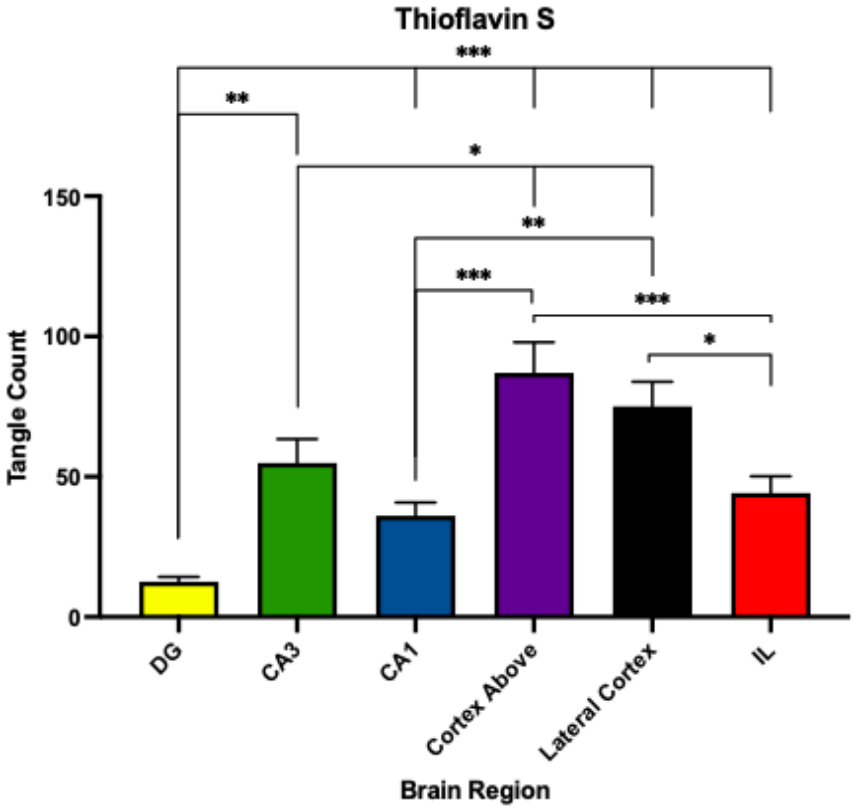

Figure 21: Thioflavin S Brain Region Differences

Figure 21 shows the differences in tangle count for the brain regions of interest for dual Tg mice which include the DG ($\bar{X}$= 12.53, *SE* =1.78), CA3 ($\bar{X}$= 54.93, *SE* =8.50), CA1 ($\bar{X}$= 36.13, *SE* = 4.71), cortex above HC ($\bar{X}$= 87.00, *SE* = 10.89), lateral cortex ($\bar{X}$= 75.00, *SE* =8.86) and IL ($\bar{X}$= 44.13, *SE* = 6.02). The DG showed the least amount of NFTs with a significantly lower tangle count than CA3 (p = .003), CA1 (p < .001), cortex above hippocampus (p < .001), lateral cortex (p < .001), and IL (p < .001) region. The cortex above hippocampus showed the greatest amount of NFTs with a significantly higher tangle count than CA3 (p = .032), CA1 (p < .001), IL (p < .001) region, and DG. The lateral cortex showed significantly greater NFTs than CA3 (p = .012), CA1 (p = .004), IL region (p = .024), and DG. Error bars indicate ± *SEM*. * indicates p < .05, ** indicates $p \leq .01$, and *** indicates $p \leq .001$.

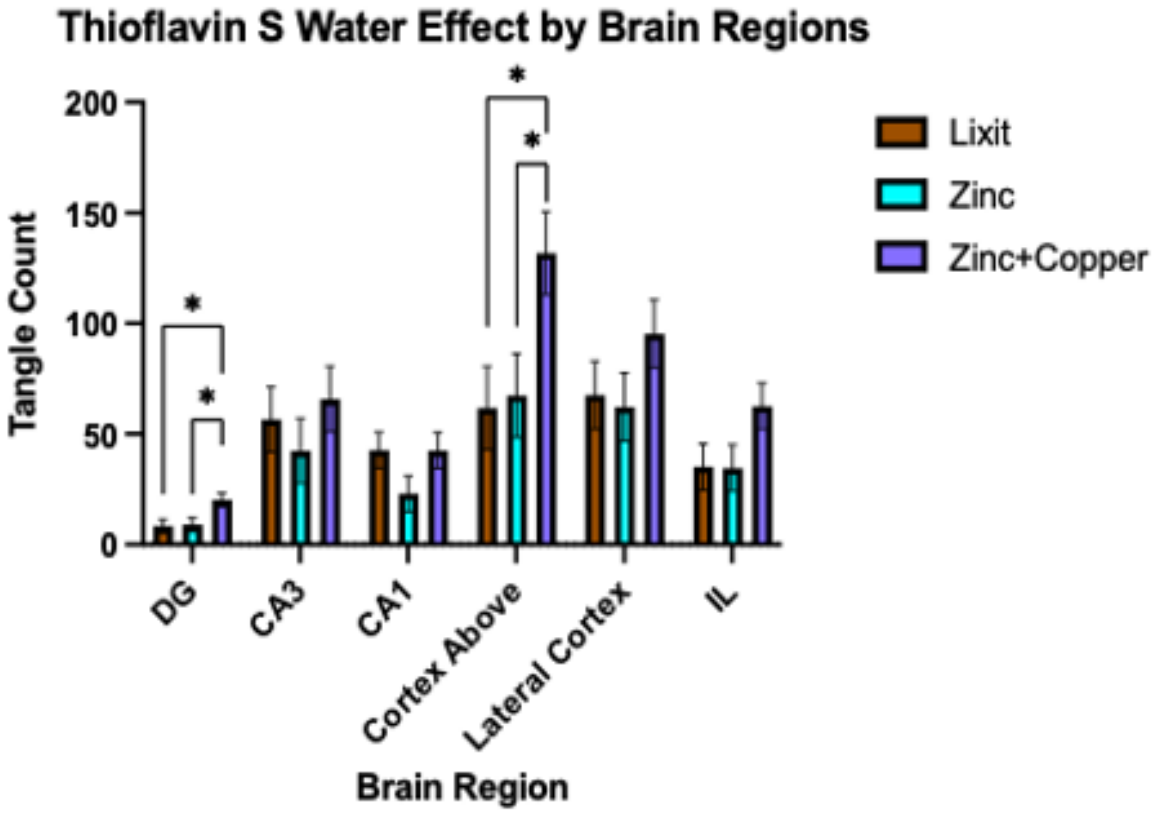

Figure 22: Thioflavin S Water Effect by Brain Region

Figure 22 shows the differences in tangle count for dual Tg mice on regular lixit, zinc, and zinc+copper water by brain region. Dual Tg mice on zinc+copper water showed a significantly higher tangle count than dual Tg mice on regular lixit (p = .019) and zinc (p = .025) water in their DG. Dual Tg mice on zinc+copper water also showed a significantly higher tangle count than dual Tg mice on regular lixit (p = .022) and zinc (p = .033) water in their cortex above HC. Graphically, dual Tg mice on zinc+copper had higher tangle counts in their CA3, lateral cortex, and IL as well, but was not statistically significant (p > .05). Error bars indicate ± *SEM*. * indicates p < .05.

CHAPTER FOUR: CONCLUSIONS

This study demonstrated the effects that zinc and zinc+copper supplementation had on the neuropathology of a dual (hAPP/htau) Tg mouse model of Alzheimer's disease. Through western blotting there showed that the dual Tg mice had significantly greater GFAP than wildtype mice. This was to be expected given that GFAP is a marker of neuroinflammation and astrocytic damage, which is released by astrocytes, and is often elevated in AD paradigms (Lippi et al., 2018). A future direction following this result would be to look at a histological plot of GFAP to see any effects on specific brain regions, as well as to compare how variations in GFAP affect variations in tau and amyloid pathology. Given the contradictory results that zinc supplementation has shown in AD mice, Zinpyr-1 staining was used as a measure to fluorescently visualize free zinc in the brain (Corona et al., 2010; Craven et al., 2018; Linkous et al., 2009; Lippi et al., 2018). Firstly, Zinpyr-1 staining showed that the wildtype mice had significantly greater free zinc than the dual Tg mice. This was consistent with the Lippi et al. (2018) study and that study explained that the reason why there would be less free zinc in the hippocampus and cortex of AD mice was that zinc has been known to attach to misfolded AD proteins. In fact, this phenomenon is thought to promote the accumulation of amyloid into plaques and prevent the clearing of these plaques (Bush, 2008). Zinc also binds to cysteine residues in tau also causing it to be inaccessible as a free ion (Lippi et al., 2018). Within

the brain regions of interests for Zinpyr-1 staining there showed significantly greater zinc in the DG than CA3, CA1, and the IL region. The IL region showed the least amount of zinc having significantly less zinc than CA1. This was also consistent with previous studies that showed high levels of zinc in the hippocampus, specifically the DG (Craven et al., 2018; Lippi et al., 2018). There did not show any fluorescence in the cortex surrounding the hippocampus and was not included in the analysis. A slight trending difference revealed that dual Tg mice on zinc water showed elevated free zinc compared to dual Tg mice on zinc+copper. Although not sufficient to reach the $p < .05$ threshold, this could suggest that by ingesting more zinc the dual Tg mice increased the levels of free zinc in their brain.

When looking at the effects zinc and zinc+copper supplementation had on amyloid plaques, there showed a significant main effect of brain regions. Upon follow up analysis there showed that the cortex above HC and IL regions had the greatest number of plaques. The cortex above HC showed significantly greater number of plaques than DG, CA3, and CA1. The IL region showed significantly more plaques than CA1. This is consistent with the Braak and Braak (1991) staging that shows hippocampal related cortex such as entorhinal and association cortex being heavily affected by amyloid plaques during the progression of AD. The infralimbic region has also been shown to interact with the hippocampus as it has been known to be involved in fear memory and interact with several limbic structures including the hippocampus (Fontanez-Nuin et al., 2011; Wood et al., 2019). A trending difference showing that the dual Tg mice on zinc+copper had less plaques than the dual Tg mice on zinc was also revealed. Upon

follow up analysis there showed that Dual Tg mice on zinc+copper water had significantly less plaques in their CA3, CA1, cortex above HC, and lateral cortex than dual Tg mice on regular lixit water. There also showed that dual Tg mice on zinc+copper had significantly less plaques in their lateral cortex and IL region than dual Tg mice on zinc water. This was more in line with the study's initial hypothesis that zinc+copper might ameliorate AD neuropathology, given that increased zinc has shown to exacerbate AD neuropathology and behavioral deficits in Tg mice (Craven et al., 2018; Linkous et al., 2009; Lippi et al., 2018; Railey et al., 2011). Given that too much zinc can lead to a copper deficiency and the fact that APP mice given zinc+copper showed performance on behavioral tests for impairment similar to control mice in the Railey et al. (2011) study, this gave a foundation to this study's initial hypothesis.

When looking at the number of NFTs via Thioflavin S stain, a significant brain regions effect was seen. Similarly, to the amyloid pathology, there showed the most NFT pathology in cortical regions. Specifically, the cortex above hippocampus showed the greatest amount of NFTs with a significantly higher tangle count than CA3, CA1, IL region, and DG. The lateral cortex showed significantly greater NFTs than CA3, CA1, IL region, and DG. Water effects were seen in specific brain regions. Specifically, dual Tg mice on zinc+copper water had a significantly higher tangle count than dual Tg mice on regular lixit and zinc water in their DG. Dual Tg mice on zinc+copper water also had a significantly higher tangle count than dual Tg mice on regular lixit and zinc water in their cortex above HC. Graphically, dual Tg mice on zinc+copper had higher tangle counts in their CA3, lateral cortex, and IL as well, but was not statistically significant. This would

suggest that zinc+copper water exacerbated NFT pathology, which goes against this study's initial hypothesis. Although, this would be in line with the behavioral study looking at these same mice under similar experimental conditions. The behavioral study using the same experimental mice, showed that dual Tg mice on zinc water showed irregular circadian rhythm activity. It also showed no significant difference between the dual Tg mice on zinc and dual Tg on zinc+copper, implying that any effect on the dual Tg mice may had just been due to zinc and not a copper deficiency (Gervase et al., 2021). The neuropathology shows that zinc+copper may have ameliorated amyloid plaque pathology, but exacerbated tau NFT pathology, which would result in no significant amelioration in behavioral deficits for the dual Tg mice given that increased tau is also related to behavioral deficits. The results in this study did not find that dual Tg mice on zinc water had greater NFTs than dual Tg mice on regular lixit water as shown by the Lippi et al. (2018) study. This also goes against the Craven et al. (2018) study which showed that a mouse model for tau pathology on zinc water showed greater NFTs than tau mice on regular lab water. The deviation from these other studies could have occurred due to a discrepancy in the levels of zinc in the zinc water. The levels of metals were measured by an environmental testing firm (TestAmerica), which showed that at one point the levels of zinc were at 8-ppm rather than 10-ppm. This might have had some effect on the number of NFTs seen for the dual Tg mice on zinc water.

Looking at the trends seen in all three histological stains, Zinpyr-1 showed the greatest levels of free zinc in the hippocampus and lowest levels in cortical regions. Congo Red showed the highest number of plaques in cortical regions and least number of

plaques in the hippocampus. Thioflavin S also showed the highest number of NFTs in cortical regions and least number of NFTs in the hippocampus. These trends make sense because the cortical regions that had the most NFTs and plaques most likely had zinc bound to them, and thus would result in less free zinc stained.

Overall, the results showing that zinc+copper might ameliorate amyloid plaque pathology and exacerbate tau NFT pathology would be consistent both with the metals hypothesis of AD and the dual pathways hypothesis, concluding that an imbalance of metals in the brain influence AD and that amyloid and tau might be more independent than suggested by the amyloid hypothesis (Bush, 2008; Small & Duff, 2008). Further investigation into "common upstream drivers" would be warranted to help explain the interaction between amyloid and tau, although there seems to be ample evidence to suggest that APOE protein might be that common upstream driver (Small & Duff, 2008). It would be interesting to see how some of these metals interact with the absence or presence of the APOE gene or its alleles in AD mice. Also, further investigation into whether metals influence Thioflavin S and Congo Red staining procedures should be considered, as Thioflavin S showed a brighter background for the dual Tg mice on zinc water for this study, while the Lippi et al. (2018) study showed small number of congophilic plaques using the same dual Tg mouse model. This would warrant antibody stains be performed to compare differences. Lastly, assessing the extent of neuronal damage and metal effects on neuronal structure in dual Tg mice through Luxol FastBlue/ Cresyl-Violet staining would also be a possible future direction.

REFERENCES

2021 Alzheimer's disease facts and figures. (2021). *Alzheimer's & Dementia*, *17*(3), 327–406. https://doi.org/10.1002/alz.12328

Allen Institute for Brain Science. (2004). Allen Mouse Brain Atlas: Coronal Atlas. *Allen Institute for Brain Science*. https://mouse.brain-map.org/static/atlas

Braak, H., & Braak, E. (1991). Neuropathological stageing of Alzheimer-related changes. *Acta Neuropathologica*, *82*(4), 239–259. https://doi.org/10.1007/BF00308809

Bush, A. I. (2008). Drug Development Based on the Metals Hypothesis of Alzheimer's Disease. *Journal of Alzheimer's Disease*, *15*(2), 223–240. https://doi.org/10.3233/JAD-2008-15208

Corona, C., Masciopinto, F., Silvestri, E., Viscovo, A. D., Lattanzio, R., Sorda, R. L., Ciavardelli, D., Goglia, F., Piantelli, M., Canzoniero, L. M. T., & Sensi, S. L. (2010). Dietary zinc supplementation of 3xTg-AD mice increases BDNF levels and prevents cognitive deficits as well as mitochondrial dysfunction. *Cell Death & Disease*, *1*, e91. https://doi.org/10.1038/cddis.2010.73

Craven, K. M., Kochen, W. R., Hernandez, C. M., & Flinn, J. M. (2018). Zinc Exacerbates Tau Pathology in a Tau Mouse Model. *Journal of Alzheimer's Disease*, *64*(2), 617–630. https://doi.org/10.3233/JAD-180151

Duce, J. A., Bush, A. I., & Adlard, P. A. (2011). Role of amyloid-b[beta]-metal interactions in Alzheimer's disease. *Future Neurology*, *6*(5), 641–659. http://dx.doi.org.mutex.gmu.edu/10.2217/fnl.11.43

Farrer, L. A., Cupples, L. A., Haines, J. L., Hyman, B., Kukull, W. A., Mayeux, R., Myers, R. H., Pericak-Vance, M. A., Risch, N., & van Duijn, C. M. (1997). Effects of Age, Sex, and Ethnicity on the Association Between Apolipoprotein E Genotype and Alzheimer Disease: A Meta-analysis. *JAMA*, *278*(16), 1349–1356. https://doi.org/10.1001/jama.1997.03550160069041

Fontanez-Nuin, D. E., Santini, E., Quirk, G. J., & Porter, J. T. (2011). Memory for Fear Extinction Requires mGluR5-Mediated Activation of Infralimbic Neurons. *Cerebral Cortex*, *21*(3), 727–735. https://doi.org/10.1093/cercor/bhq147

Gervase, T. N., Booth, A., Neff, S., Hoyos Justiniano, R., Lamarche, M. S., Allen, L. E., & Flinn, J. M. (2021). *Examining behavior of a double transgenic (APP/tau) mouse model of Alzheimer's disease on zinc and copper supplementation*.

Hsiao, K., Chapman, P., Nilsen, S., Eckman, C., Harigaya, Y., Younkin, S., Yang, F., & Cole, G. (1996). Correlative Memory Deficits, Aβ Elevation, and Amyloid Plaques in Transgenic Mice. *Science, New Series*, *274*(5284), 99–102.

Kumar, A., Singh, A., & Ekavali. (2014). A review on Alzheimer's disease pathophysiology and its management: An update. *Pharmacological Reports*, *67*(2), 195–203. https://doi.org/10.1016/j.pharep.2014.09.004

Linkous, D. H., Adlard, P. A., Wanschura, P. B., Conko, K. M., & Flinn, J. M. (2009). The Effects of Enhanced Zinc on Spatial Memory and Plaque Formation in

Transgenic Mice. *Journal of Alzheimer's Disease*, *18*(3), 565–579. https://doi.org/10.3233/JAD-2009-1162

Lippi, S. L. P., Smith, M. L., & Flinn, J. M. (2018). A Novel hAPP/htau Mouse Model of Alzheimer's Disease: Inclusion of APP With Tau Exacerbates Behavioral Deficits and Zinc Administration Heightens Tangle Pathology. *Frontiers in Aging Neuroscience*, *10*. https://doi.org/10.3389/fnagi.2018.00382

Maret, W., & Sandstead, H. H. (2006). Zinc requirements and the risks and benefits of zinc supplementation. *Journal of Trace Elements in Medicine and Biology: Organ of the Society for Minerals and Trace Elements (GMS)*, *20*(1), 3–18. https://doi.org/10.1016/j.jtemb.2006.01.006

Nations, S. P., Boyer, P. J., Love, L. A., Burritt, M. F., Butz, J. A., Wolfe, G. I., Hynan, L. S., Reisch, J., & Trivedi, J. R. (2008). Denture cream: An unusual source of excess zinc, leading to hypocupremia and neurologic disease. *Neurology*, *71*(9), 639–643. https://doi.org/10.1212/01.wnl.0000312375.79881.94

O'Brien, R. J., & Wong, P. C. (2011). Amyloid Precursor Protein Processing and Alzheimer's Disease. *Annual Review of Neuroscience*, *34*, 185–204. https://doi.org/10.1146/annurev-neuro-061010-113613

Railey, A. M., Groeber, C. M., & Flinn, J. M. (2011). The Effect of Metals on Spatial Memory in a Transgenic Mouse Model of Alzheimer's Disease. *Journal of Alzheimer's Disease*, *24*(2), 375–381. https://doi.org/10.3233/JAD-2011-101452

Railey, A. M., Micheli, T. L., Wanschura, P. B., & Flinn, J. M. (2010). Alterations in fear response and spatial memory in pre- and post-natal zinc supplemented rats:

Remediation by copper. *Physiology & Behavior*, *100*(2), 95–100. https://doi.org/10.1016/j.physbeh.2010.01.040

Small, S. A., & Duff, K. (2008). Linking Aβ and Tau in Late-Onset Alzheimer's Disease: A Dual Pathway Hypothesis. *Neuron*, *60*(4), 534–542. https://doi.org/10.1016/j.neuron.2008.11.007

Sun, A., Nguyen, X. V., & Bing, G. (2002). Comparative Analysis of an Improved Thioflavin-S Stain, Gallyas Silver Stain, and Immunohistochemistry for Neurofibrillary Tangle Demonstration on the Same Sections. *Journal of Histochemistry & Cytochemistry*, *50*(4), 463–472. https://doi.org/10.1177/002215540205000403

Wood, M., Adil, O., Wallace, T., Fourman, S., Wilson, S. P., Herman, J. P., & Myers, B. (2019). Infralimbic prefrontal cortex structural and functional connectivity with the limbic forebrain: A combined viral genetic and optogenetic analysis. *Brain Structure & Function*, *224*(1), 73–97. https://doi.org/10.1007/s00429-018-1762-6

BIOGRAPHY

Rafael Hoyos Justiniano graduated from Thomas A. Edison High School in Alexandria, Virginia in 2016. He received his Bachelor of Science in Neuroscience with a minor in Psychology from George Mason University in 2020. He was employed as a Graduate Teaching Assistant, teaching an upper-level undergraduate lab course called Biopsychology Laboratory, and as Graduate Professional Assistant in Latinx Advocacy and Outreach while working towards his Master of Arts in Psychology with a concentration in Cognitive and Behavioral Neuroscience from George Mason University.